

Thermodynamic analogy for quantum phase transitions at zero temperature

Pavel Cejnar^a, Stefan Heinze^b, Jan Dobeš^c

^a*Institute of Particle and Nuclear Physics, Charles University, V Holešovičkách 2, 180 00 Prague, Czech Republic*

^b*Institute of Nuclear Physics, University of Cologne, Zùlpicherstrasse 77, 50937 Cologne, Germany*

^c*Nuclear Physics Institute, Academy of Sciences of the Czech Republic, 250 68 Řež, Czech Republic*

Abstract

We propose a relationship between thermodynamic phase transitions and ground-state quantum phase transitions in systems with variable Hamiltonian parameters. It is based on a link between zeros of the canonical partition function at complex temperatures and exceptional points of a quantum Hamiltonian in the complex-extended parameter space. This approach is applied in the interacting boson model, where it is shown to properly distinguish the first- and second-order phase transitions.

Key words: Quantum phase transitions, Exceptional points, Zeros of partition function

PACS: 05.70.Fh, 21.60.Ev

1 Introduction

Quantum phase transitions (QPT's) are now a well documented phenomenon in both lattice [1] and many-body systems [2,3,4,5,6,7,8,9,10,11,12,13,14,15]. A QPT Hamiltonian usually reads as a superposition of two incompatible terms,

$$H(\lambda) = H_0 + \lambda V = (1 - \lambda)H(0) + \lambda H(1) , \quad (1)$$

$[H_0, V] \neq 0$, where $\lambda \in [0, 1]$ is a dimensionless control parameter that drives the system between two limiting modes of motions. It can be shown that

the ground-state (g.s.) average $\langle V \rangle_0 \equiv \langle \Psi_0(\lambda) | V | \Psi_0(\lambda) \rangle$ is a nonincreasing function of λ . In the QPT situation it evolves in such a way that either $\langle V \rangle_0$ itself or some of its derivatives change discontinuously (for infinite system's size) at a certain critical value λ_c .

Of particular interest are the cases when $\langle V \rangle_0$ drops to zero and, simultaneously, also $\langle V^2 \rangle_0 = 0$ at the critical point. Then the g.s. wave function $|\Psi_0(\lambda)\rangle$ gets fixed for all $\lambda \geq \lambda_c$ and $\langle V \rangle_0$ plays a role of an “order parameter” whose value (zero or nonzero) distinguishes two quantum “phases” of the model. This scenario is realized in various many-body models, mostly known from nuclear physics. Limits $H(0)$ and $H(1)$ are usually connected with collective or single-particle motions corresponding to spherical and deformed nuclear shapes [2,3,4,5,6,8,9,10,11,12,13], but they can also represent paired and unpaired fermionic phases of nuclei [4,5,7,14], or normal and superradiant modes of interacting atom-field systems [15].

Questions often arise concerning the depth to which the term “phase transition” can be followed in the direction of standard thermodynamics. Or is it only a metaphor? The g.s. QPT's in the sense of Eq. (1) happen at zero temperature and thus have no real thermal attributes. Nevertheless, as discussed in Refs.[10,13,14,16], counterparts of some thermodynamic terms can often be derived from standard quantum-mechanical expressions. A unified thermodynamic-like approach to characterize the QPT situation is, however, missing.

In this Letter, we present a method capable to establish the thermodynamic analogy for quantum phase transitions on a new, general basis. The method relates zeros of the canonical partition function $Z(T)$ at complex temperatures T [17,18,19] to exceptional, or branch points of Hamiltonian (1) in complex-extended λ plane [5,20,21,22,23,24,25]. This link is not artificial. While neither zeros, nor exceptional points occur on the real T or λ axes in the finite case (this would imply divergences of thermodynamic observables or real crossings of quantum levels, which are generically forbidden), it is known that their distribution in the complex plane determines the key features of the system in the physical (real) domain. Zeros and exceptional points thus play crucial roles also in the fundamental theory of classical and quantum phase transitions. Indeed, places where in the thermodynamic limit the complex zeros of $Z(T)$ approach infinitely close to the real T -axis can be identified with points of classical phase transitions [17,18,19], while similar convergence of exceptional points to real λ induces singular evolution of energies and wave functions, as observed in $T = 0$ quantum phase transitions [5,24].

2 QPT analog of specific heat

One obvious way to quantitatively exploit the thermodynamic analogy relies on connecting the g.s. energy, $E_0(\lambda)$, as a function of the interaction parameter λ , with the equilibrium value of a thermodynamic potential, $F_0(T)$, as a function of temperature T (an alternative link to the inverse temperature β would not result in qualitative differences). From the relation $\langle V \rangle_0 = dE_0/d\lambda$ it follows that if the $(l-1)$ -th derivative of $\langle V \rangle_0$ is discontinuous at λ_c , then derivatives of the g.s. energy are discontinuous starting from $d^l E_0/d\lambda^l$ so that the QPT is of the l -th order [3]. The ‘‘specific heat’’ defined through the second derivative of E_0 in such a transition (in analogy to standard definition $C = -T\partial^2 F_0/\partial T^2$)

$$C_1 = -\lambda \frac{d^2 E_0}{d\lambda^2} = -\lambda \frac{d\langle V \rangle_0}{d\lambda} = 2\lambda \sum_{i>0} \frac{|\langle \Psi_i | V | \Psi_0 \rangle|^2}{E_i - E_0} \quad (2)$$

behaves exactly as expected for a thermodynamic phase transition of the same order. Here, $E_i(\lambda)$ and $|\Psi_i(\lambda)\rangle$ are the i -th energy and eigenvector, respectively.

This relation can be easily verified [13] in the interacting boson model (IBM) [26], where both first- and second-order phase transitions between spherical and deformed g.s. shapes are present in the parameter space [2,3,6,8,9,10,11,12,13]. The model describes shapes and collective motions of atomic nuclei in terms of an ensemble of N interacting s and d bosons with angular momenta 0 and 2, respectively. We employ a simplified IBM Hamiltonian [8,9,10,11,12,13]

$$H(\lambda) = (1 - \lambda) \left[-\frac{q_\chi \cdot q_\chi}{N} \right] + \lambda n_d \quad (3)$$

where $n_d = d^\dagger \cdot \tilde{d}$ is the d -boson number operator, and $q_\chi = d^\dagger \tilde{s} + s^\dagger \tilde{d} + \chi (d^\dagger \tilde{d})^{(2)}$ the quadrupole operator. In the $N \rightarrow \infty$ limit, the order parameter $\langle V \rangle_0/N$ (normalization per boson is necessary to deal with effects of varying N) can be expressed in terms of the g.s. deformation parameter β_0 [2]:

$$\lim_{N \rightarrow \infty} \frac{\langle V \rangle_0}{N} = \frac{5\beta_0^2 - 4\sqrt{\frac{2}{7}}\chi\beta_0^3 + \left(\frac{2}{7}\chi^2 + 1\right)\beta_0^4}{(1 + \beta_0^2)^2}. \quad (4)$$

For $\chi \neq 0$, the value of β_0 drops from a nonzero value β_{0c} to 0 at $\lambda = \lambda_c(\chi) = (4 + 2\chi^2/7)/(5 + 2\chi^2/7)$, indicating a first-order deformed-spherical QPT. For $\chi = 0$, the value $\beta_0 \propto \sqrt{\lambda_c - \lambda}$ valid in the left vicinity of the critical point $\lambda_c(0)$ continuously joins with $\beta_0 = 0$ valid above λ_c ; the corresponding QPT is of the second order. In both cases $\langle V^2 \rangle_0/N \rightarrow 0$ for $\lambda > \lambda_c$ and $N \rightarrow \infty$.

The dependence of C_1 on λ in the phase-transitional region is shown in Fig. 1 for various boson numbers N . Panels (a) and (b) correspond to $\chi = -\sqrt{7}/2$ and 0, respectively. With an increasing size of the system, the specific heat in panel (a), normalized per boson, would form a δ -function singularity in the $N \rightarrow \infty$ limit (first-order QPT), while C_1/N derived from panel (b) would develop just a discontinuity at λ_c (second-order QPT). Note that using the asymptotic $E_0(\lambda)/N \leftrightarrow F_0(T)$ correspondence, one can moreover show that the IBM shape-phase diagram fully agrees with the classical Landau theory of thermodynamic phase transitions [12].

3 QPT distribution of exceptional points

Exceptional points of Hamiltonian (1) are points in the complex plane of parameter λ where various pairs of eigenvalues of the complex-extended Hamiltonian coalesce. They are simultaneous solutions of equations $\det[E - H(\lambda)] = 0$ and $(\partial/\partial E) \det[E - H(\lambda)] = 0$, which after elimination yield the following condition [20,23]:

$$D(\lambda) = \prod_k D_k(\lambda) = - \prod_{i < j} [E_j(\lambda) - E_i(\lambda)]^2 = 0, \quad (5)$$

$$D_k(\lambda) = \prod_{i(\neq k)} [E_i(\lambda) - E_k(\lambda)]. \quad (6)$$

The discriminant $D(\lambda)$ is a polynomial of order $n(n-1)$ in λ (where n is the dimension of the Hilbert space) with real coefficients and its roots thus occur as $n(n-1)/2$ complex conjugate pairs. Except at these points, the complex energy $E(\lambda)$ obtained from the characteristic polynomial of Hamiltonian (1) is a single analytic function defined on n Riemann sheets. The energy labels in Eqs. (5) and (6) enumerate the respective Riemann sheet according to the ordering of energies at real λ . Exceptional points are square-root branch points where the Riemann sheets are pairwise connected. The leading-order behavior on the two connected sheets close to the branch point λ_0 is given by $E(\lambda) - E(\lambda_0) \approx a\sqrt{\lambda - \lambda_0}$ (as a doubly-valued function), with a being a complex constant [5,21,23].

The relation of exceptional points to quantum phase transitions has been declared several times—see, e.g., Refs. [5,9,24]. Clearly, an exceptional point located close to the real λ axis affects the local evolution of the corresponding pair of real energies so that the two levels undergo an avoided crossing with accompanying rapid changes of wave functions. A cumulation of exceptional points close to some real point λ_c thus can give rise to massive structural changes of eigenstates, as observed in QPT's. Although this mechanism was

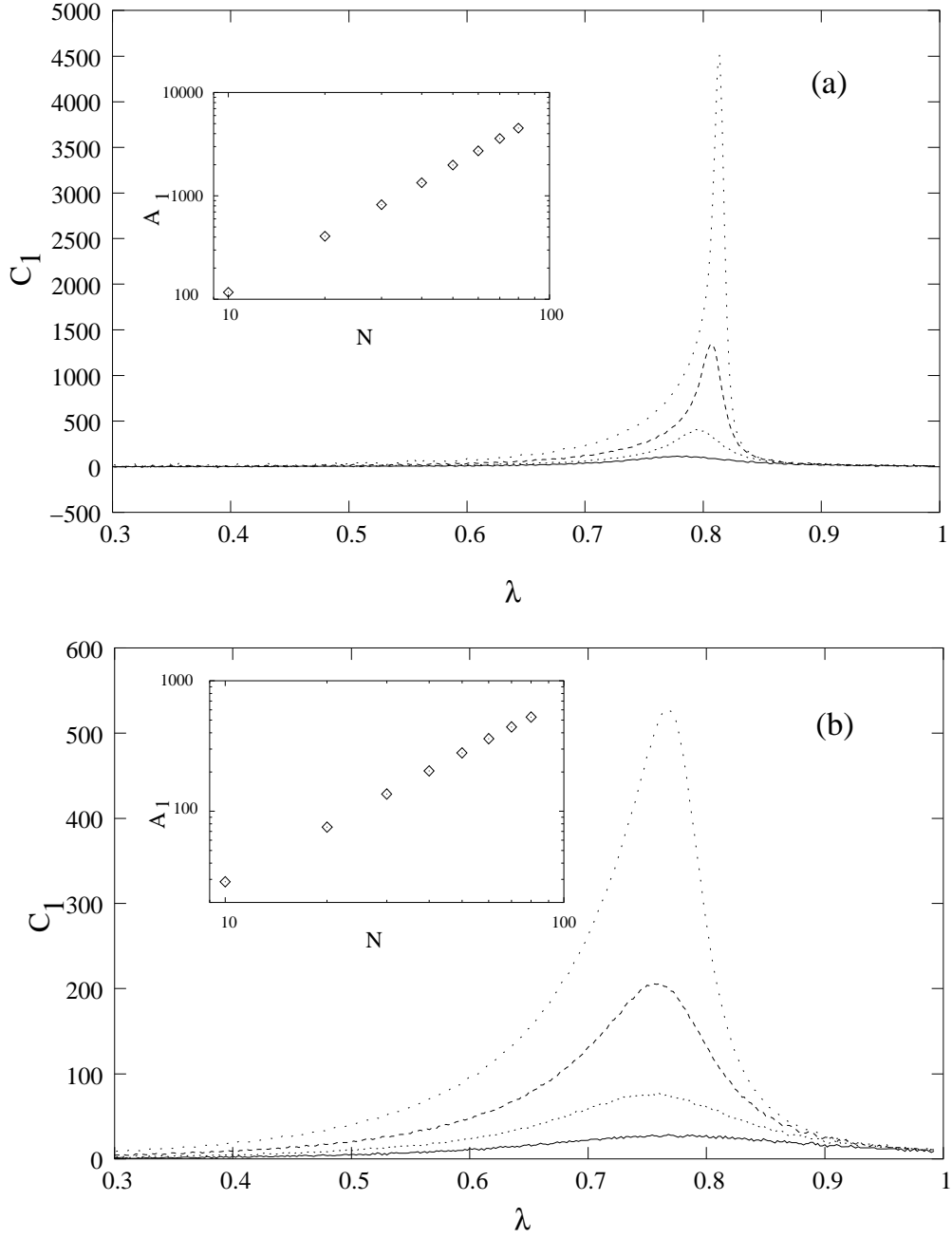


Fig. 1. “Specific heat” (2) in the first-order (panel a) and second-order (panel b) QPT of the interacting boson model [Hamiltonian (3) with (a) $\chi = -\sqrt{7}/2$ and (b) $\chi = 0$]. The curves, in order from the lowest to the highest, correspond to $N = 10, 20, 40,$ and $80,$ respectively; the insets show the increase of the maximal value with N .

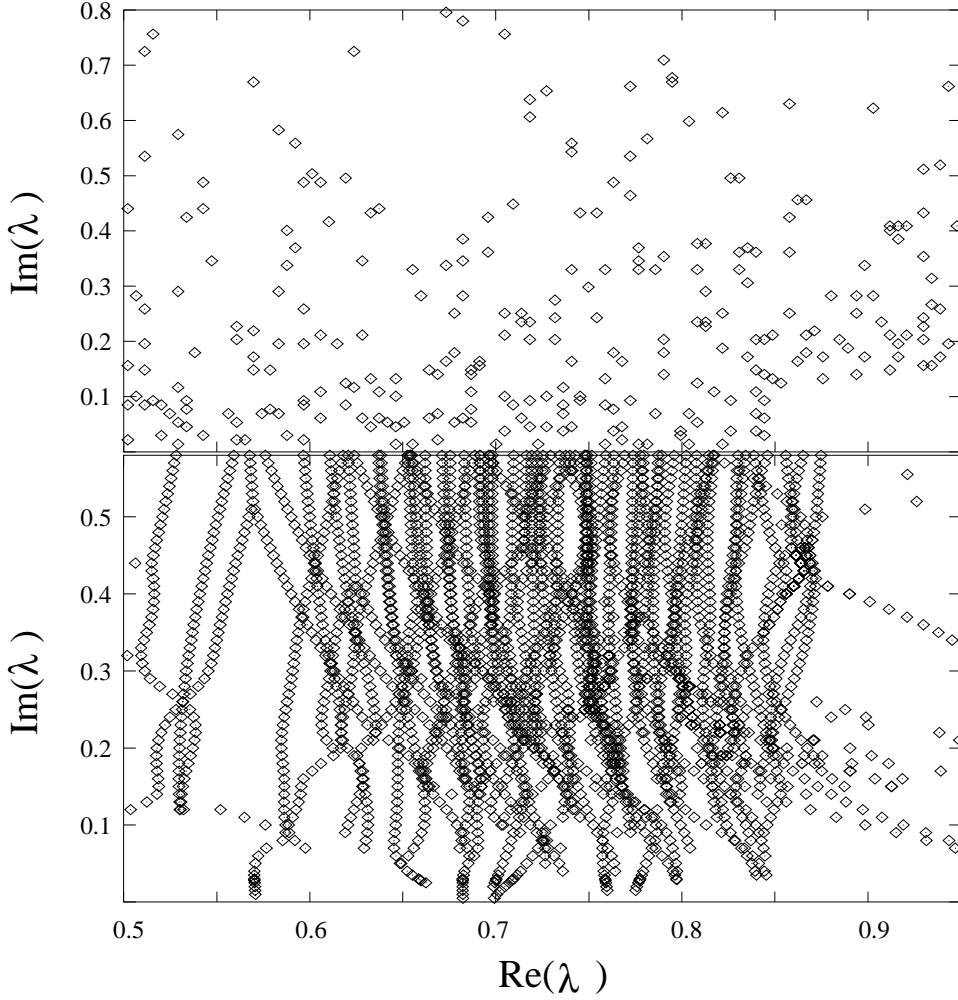


Fig. 2. Exceptional points (upper panel) and crossings of energy real parts (lower panel) in complex λ plane for $J = 0$ eigenstates of Hamiltonian (3) with $\chi = -\sqrt{7}/2$ and $N = 20$. Only the lowest 10 levels out of $n = 44$ are included in the lower panel.

illustrated by several model examples [5,24], quantitative determination of the arrangement and density of exceptional points needed to trigger a phase-transitional behavior is still missing.

Exceptional points for levels with angular momentum $J = 0$ in the vicinity of the IBM first- and second-order phase transitions are for $N = 20$ shown in the upper panels of Figs. 2 and 3, respectively. The calculation was done using the method described in Ref.[20]. Lower panels of both figures display—for the lowest ten levels, ordered according to $\text{Re}E_i$ —lines where energy real parts of two different levels cross, i.e., satisfy $\text{Re}E_i(\lambda) = \text{Re}E_j(\lambda)$. As follows from the square-root behavior of energies close to crossings, the endpoints of these lines coincide with starting points of the $\text{Im}E_i(\lambda) = \text{Im}E_j(\lambda)$ lines (not shown here), so they represent the exceptional points.

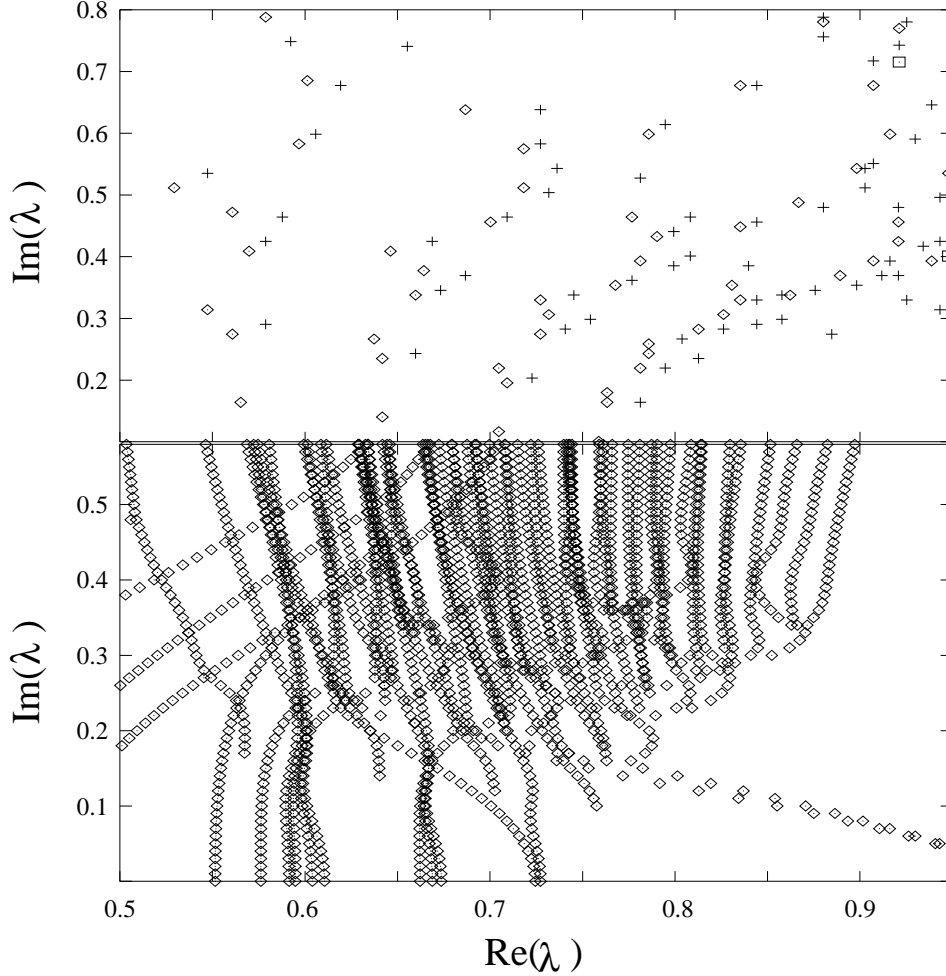


Fig. 3. The same as in Fig. 2, but for $\chi = 0$. In this case, single exceptional points (diamonds) coexist with doubly and even quadruply degenerate ones (crosses and rectangles, respectively).

Several exceptional points in Fig. 3 apparently lie on the real λ -axis. This results from the underlying $O(5)$ dynamical symmetry of Hamiltonian (3) for $\chi = 0$, with the seniority quantum number ν , that survives all the way across the transition and thus enables the levels with the same J to cross on the real axis [27]. Nongeneric features implied by the additional symmetry at $\chi = 0$ also include double or even higher degeneracy of some exceptional points observed (within the available numerical precision) in Fig. 3.

Broad distributions of exceptional points in Figs. 2 and 3 do not seem to indicate the QPT behavior at $\lambda \approx 0.8$, but it must be stressed that these figures contain points belonging to various Riemann sheets, while only the ground-state Riemann sheet is relevant in the present case. Unfortunately, to attribute the points to the respective sheets through the available numerical data becomes problematic already for relatively small dimensions and the

study of effects connected with increasing boson numbers seems intractable.

4 Alternative definition of a QPT specific heat

The above problem can be approached via the relation of the ground-state related exceptional points to zeros of partition function. We will use the correspondence $Z(T) \leftrightarrow D_0(\lambda)$ between the partition function and $k = 0$ partial discriminant (6). In fact, the square D_k^2 of any partial discriminant is a polynomial with $n - 1$ complex conjugate pairs of roots, each of them being simultaneously assigned to one other $D_{k'}$. These roots correspond to the branch points located on the k -th Riemann sheet, so that zeros of D_0 represent singularities on the ground-state Riemann sheet. A counterpart of the thermodynamic potential $F_0 = -T \ln Z$ is proportional to the g.s. “potential energy”, $U = -\sum_{i>0} \ln |E_i - E_0|$, as obtained in the static Coulomb-gas model for quantum energy levels [28]. The divergence of U (zero of D_0) implies an infinite “force” on the ground state also in the dynamical Pechukas-Yukawa model [29]. For the “specific heat” one obtains (in analogy with the standard formula $C = T^2 \partial^2 \ln Z / \partial T^2 + 2T \partial \ln Z / \partial T$)

$$C_2 = S \sum_{i>0} \left[\lambda^2 \left\{ \frac{\frac{d^2 E_i}{d\lambda^2} - \frac{d^2 E_0}{d\lambda^2}}{E_i - E_0} - \left(\frac{\frac{dE_i}{d\lambda} - \frac{dE_0}{d\lambda}}{E_i - E_0} \right)^2 \right\} + 2\lambda \left(\frac{\frac{dE_i}{d\lambda} - \frac{dE_0}{d\lambda}}{E_i - E_0} \right) \right]. \quad (7)$$

One can equivalently use $C_2 = -S\lambda d^2(\lambda U)/d\lambda^2$, which is the same as Eq. (2), but with E_0 replaced by λU . Note that an arbitrary power of D_0 used in the thermodynamic correspondence would modify just the overall scaling factor S . This factor must also depend on the size of the system (similarly as the thermodynamic specific heat is normalized to a mass unit) and will be discussed later. Eq. (7) can be further decomposed [29] into a double sum of terms containing energy differences (in denominators) and matrix elements of V (in numerators), cf. Eq. (2).

Although the quantity C_2 depends solely on real- λ spectral observables, its behavior in a QPT is an indirect measure of the density of exceptional points on the ground-state Riemann sheet beyond (but close to) the real axis. Consider, for instance, a chain $\lambda_{\pm m} = \lambda_c \pm i\tilde{\lambda}_m$ of D_0 zeros along a line perpendicular to the real axis. The D_0^2 polynomial is determined (up to a multiplicative constant) by the roots and specific heat (7) is for real λ given by

$$C_2 \propto \lambda^2 \int_0^\infty \frac{\rho(\tilde{\lambda})(\tilde{\lambda}^2 - \Delta^2)}{(\tilde{\lambda}^2 + \Delta^2)^2} d\tilde{\lambda} + 2\lambda\Delta \int_0^\infty \frac{\rho(\tilde{\lambda})}{\tilde{\lambda}^2 + \Delta^2} d\tilde{\lambda}, \quad (8)$$

where $\Delta = \lambda - \lambda_c$ and $\rho(\tilde{\lambda})$ is a density of exceptional points along the $\lambda_c + i\tilde{\lambda}$ line. This implies that the “latent heat” $Q = \lim_{\epsilon \rightarrow 0} \int_{-\epsilon}^{+\epsilon} C_2(\Delta) d\Delta$ is equal to zero if $\rho(\tilde{\lambda})$ decreases sufficiently fast when approaching the real axis. In particular, if $\rho(\tilde{\lambda}) \sim \tilde{\lambda}^\alpha$ for $\tilde{\lambda} \rightarrow 0$, we obtain the following possibilities: (i) a first-order QPT, with $C_2 \rightarrow \infty$ at $\Delta = 0$ and Q finite, for $\alpha = 0$, (ii) second-order QPT, with $C_2 \rightarrow \infty$ but $Q = 0$, for $\alpha \in (0, 1]$, and (iii) a higher-order QPT, with C_2 finite and $Q = 0$, for $\alpha > 1$. This relation is the same as in standard thermodynamics, where the order of a phase transition reflects the density of the $Z(T)$ zeros close to a critical temperature T_c [18]. It should be stressed, however, that in the QPT case the order deduced from C_2 cannot be *a priori* expected to coincide with the order determined via C_1 . We will focus on this problem in the following, using the IBM.

The specific heat C_2 in the IBM first- and second-order QPT is for $S = 1$ shown in Fig. 4, where panels (a) and (b) again correspond to $\chi = -\sqrt{7}/2$ and 0, respectively. All the levels with $J = 0$ were included in the sum (7). We know that for $\chi = 0$ some pairs of levels actually cross at real λ (due to the seniority quantum number v). This implies discontinuities and singularities of the first and second derivatives in Eq. (7), which however cancel out exactly and do not affect the C_2 shape in Fig. 4(b).¹

It is clear that the peaks in panels (a) of both Figs. 1 and 4 are sharper and higher than those in panels (b), as indeed expected in the first- and second-order phase transitions. The log-log insets in these figures indicate that maximal values— A_1 and A_2 —in the C_1 and C_2 peaks exhibit roughly an algebraic increase with the boson number. The increase is faster for the first-order QPT than for the second-order one. We will show that with a proper normalization to the system’s size, the values of A_1 and A_2 corresponding to the second-order QPT have a finite $N \rightarrow \infty$ asymptotics, while the values of the first-order QPT, normalized in the same way, diverge.

Fig. 5 shows the dependence of A_1/N and A_2/N^2 for the second-order QPT on the boson number up to $N = 1000$. The calculation for such high dimensions was enabled by the underlying $O(5)$ symmetry for $\chi = 0$. Clearly, the curves in Fig. 5 have finite asymptotics. The behavior of A_1 is consistent with the analytic result $A_1/N \rightarrow 12.5$ that can be derived from the $N \rightarrow \infty$ limit of the g.s. energy per boson. The faster increase of A_1 in the first-order transition, see Fig. 1(a), indicates a divergence of C_1/N at $\lambda_c(\chi)$ for $\chi \neq 0$.

¹ If E_i crosses with E_{i+1} , the discontinuity (singularity) of the first (second) derivatives in Eq. (7) for both levels is the same, but with opposite signs, so the sum of both contributions is incremented correctly, as if the levels continuously passed the crossing.

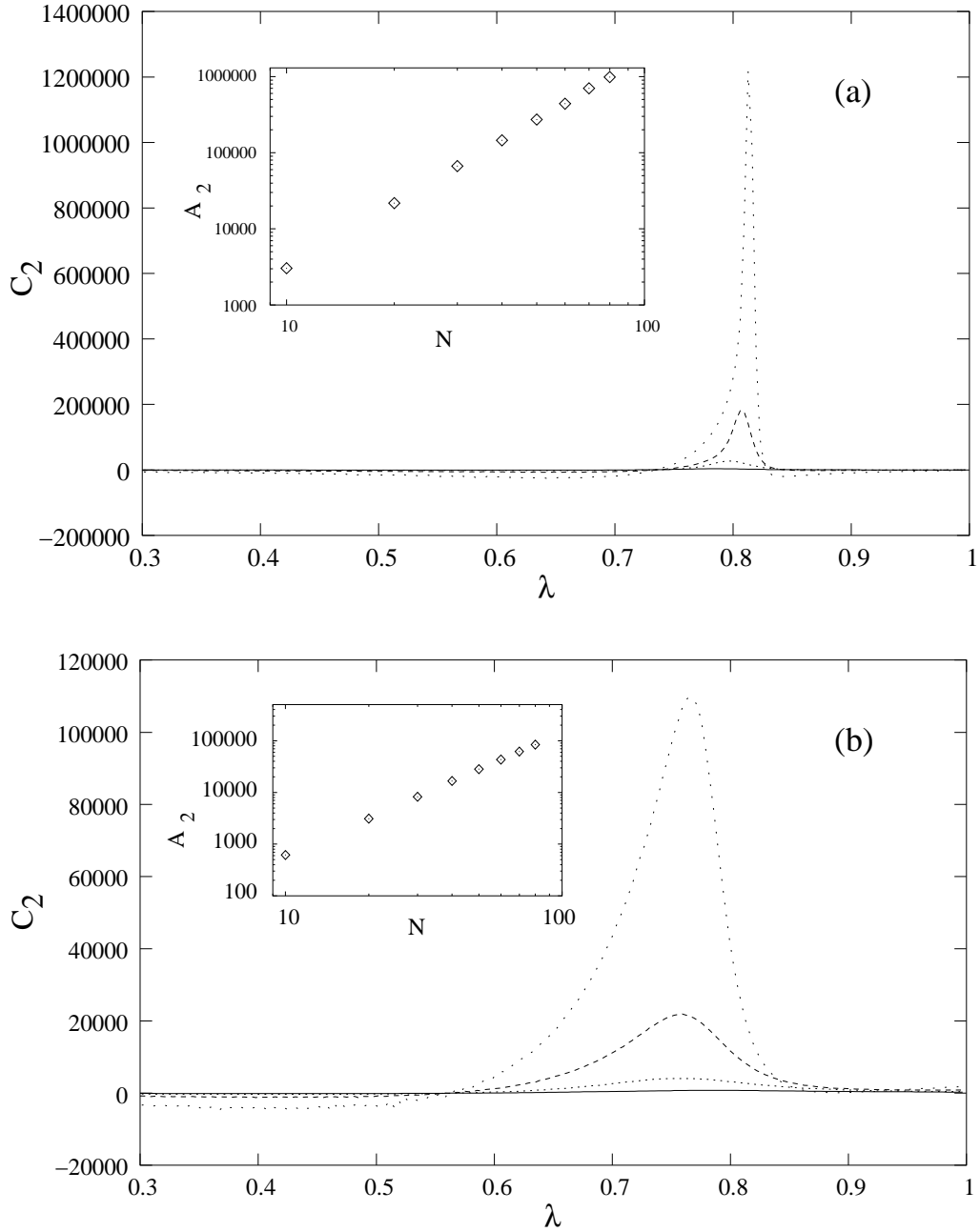


Fig. 4. The same as in Fig. 1 but for “specific heat” (7) including all $J = 0$ states.

Specific heat C_2 in Fig. 4 behaves in a similar way, but—as follows from Fig. 5—in this case the correct normalization is by $1/N^2$. This factor reflects the dimension of the subspace of states with $J = 0$ which grows roughly as $n \sim N^2/12$ for very large boson numbers (while the total number of IBM states is $\sim N^5/120$). Since there are $n - 1$ pairs of exceptional points on each Riemann sheet, the choice of $S = 1/(n - 1) \propto 1/N^2$ in Eq. (7) normalizes the density $\rho(\tilde{\lambda})$ [cf. Eq. (8)] in the finite- n case to a unit integral and plays a similar role

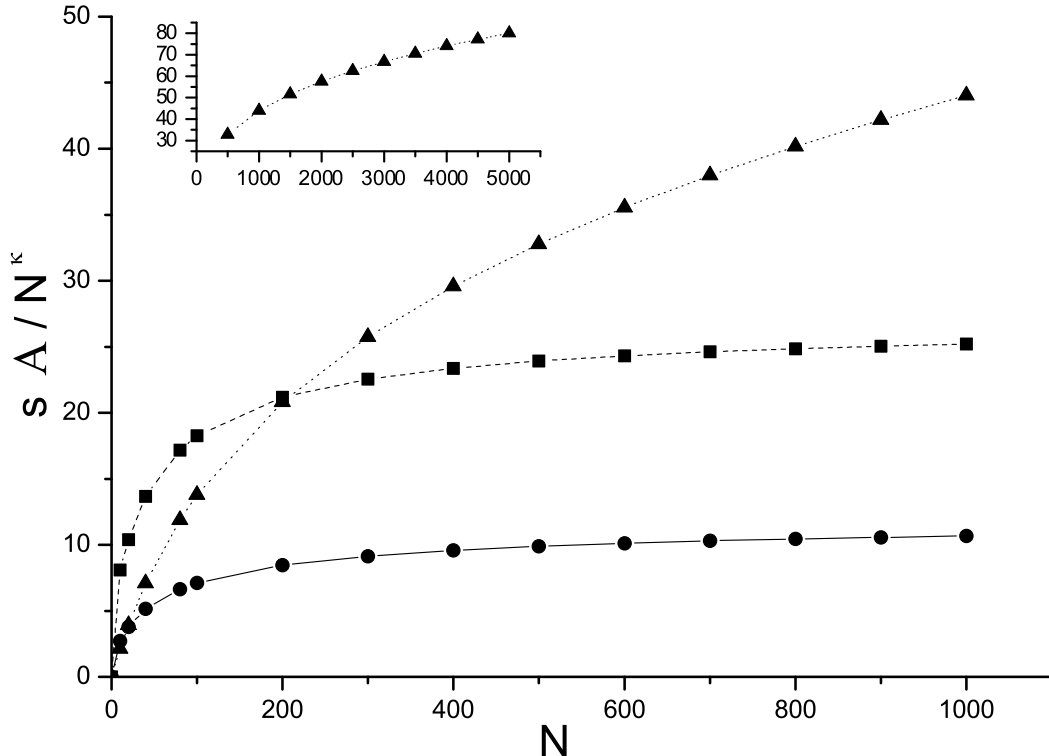


Fig. 5. Normalized maximal values A_1/N (dots), s_2A_2/N^2 (rectangles), and $s'_2A'_2/N$ (triangles) of “specific heat” (2) and (7) in the IBM second-order QPT ($\chi = 0$) for very large boson numbers. A_2 and A'_2 were obtained using the whole $J = 0$ space or only its $v = 0$ subspace, respectively. The behavior of A'_2 up to $N = 5000$ is shown in the inset. Scaling factors $s_2 = 10$ and $s'_2 = 0.5$ were used just to show all data within the same range.

as the $1/N$ scaling of C_1 in the previous case. With this normalization, the specific heat C_2 correctly distinguishes the IBM first- and second-order phase transitions.

This conclusion is also supported by the analysis of the IBM classical limit. Indeed, due to the degeneracy of $\beta_0 = 0$ and $\beta_0 \neq 0$ minima of the $N \rightarrow \infty$ g.s. energy per boson at λ_c [2], there is an exceptional point on the ground-state Riemann sheet that is for the infinite boson number located on the real axis, at the first-order QPT. Consequently, energy denominators in Eq. (7) diverge at this point in a way that appears to be faster than $\propto N^2$. In contrast, there is no actual ground-state involving degeneracy in the asymptotic limit of the second-order transition, although, as can be shown, exceptional points come infinitely close to the real axis at the critical point. This results in a slower increase, which is compensated by the $1/N^2$ scaling.

For $\chi = 0$, we can additionally check the validity of the $S = 1/(n - 1)$ normalization of specific heat (7) by considering only the $v = 0$ subspace of $J = 0$ states, with the dimension $n \sim N/2$. Since this subspace contains the

ground state and does not mix with $v \neq 0$ subspaces, one can restrict the sum in Eq. (7) only to these states and obtain a modified specific heat C'_2 . It is expected to have a similar behavior as C_2 , but with $S \propto 1/N$. Unfortunately, the convergence of the maximal value A'_2 to some asymptotics is very slow. The available data for boson numbers up to 5000 (see the inset in Fig. 5) can only yield an upper constraint for the power in $S \propto 1/N^\kappa$, namely $\kappa < 1.35$, which is consistent with the expectation but not fully conclusive. Work in this direction is in progress.

5 Conclusions

We have developed a method capable to indirectly measure the distribution of exceptional points of Hamiltonian (1) on the ground-state Riemann sheet near the real- λ axis. This distribution plays major role in structural changes of the g.s. wave function. It is crucial in the determination of zero-temperature quantum phase transitions, but numerically difficult to be calculated directly for large dimensions. The method is based on the analogy between generic QPT arrangements of exceptional points and similar behaviors of complex zeros of the canonical partition function in thermodynamic phase transitions. The resulting formula (7) for the “specific heat” C_2 normalized with respect to the relevant dimension, $S \sim 1/n$, turned out to be the appropriate measure for the cumulation of exceptional points near the QPT critical point. Our approach was tested in the interacting boson model, where C_2 in the first- and second-order QPT’s was shown to behave in the same way as standard specific heat in typical thermodynamic phase transitions of the respective orders. We expect that the method is applicable also in other QPT systems, even beyond nuclear physics. It discloses surprising analogy between standard thermodynamics and quantum mechanics of parameter-dependent systems.

Acknowledgments

P.C. and S.H. thank Jan Jolie for relevant discussions. This work was supported by GAČR and ASČR under Project Nos. 202/02/0939 and K1048102, respectively, and by the DFG under Grant No. 436 TSE 17/6/03.

References

- [1] S. Sachdev, *Quantum Phase Transitions* (Cambridge University Press, Cambridge, UK, 1999).

- [2] A.E.L. Dieperink, O. Scholten, and F. Iachello, Phys. Rev. Lett. 44 (1980) 1747; A.E.L. Dieperink, O. Scholten, Nucl. Phys. A346 (1980) 125.
- [3] D.H. Feng, R. Gilmore, S.R. Deans, Phys. Rev. C 23 (1981) 1254.
- [4] W.-M. Zhang, D.H. Feng, J.N. Ginocchio, Phys. Rev. Lett. 59 (1987) 2032; Phys. Rev. C 37 (1988) 1281; W.-M. Zhang, C.-L. Wu, D.H. Feng, J.N. Ginocchio, M.W. Guidry, *ibid.* 38 (1988) 1475.
- [5] W.D. Heiss, Z. Phys. A - Atomic Nuclei 329 (1988) 133; W.D. Heiss, A.L. Sannino, Phys. Rev. A 43 (1991) 4159; W.D. Heiss, Phys. Rep. 242 (1994) 443.
- [6] E. López-Moreno, O. Castaños, Phys. Rev. C 54 (1996) 2374.
- [7] D.J. Rowe, C. Bahri, W. Wijesundera, Phys. Rev. Lett. 80 (1998) 4398; C. Bahri, D.J. Rowe, W. Wijesundera, Phys. Rev. C 58 (1998) 1539.
- [8] R.F. Casten, D. Kusnezov, N.V. Zamfir, Phys. Rev. Lett. 82 (1999) 5000.
- [9] P. Cejnar, J. Jolie, Phys. Rev. E 61 (2000) 6237.
- [10] P. Cejnar, V. Zelevinsky, V.V. Sokolov, Phys. Rev. E 63 (2001) 036127.
- [11] J. Jolie, R.F. Casten, P. von Brentano, V. Werner, Phys. Rev. Lett. 87 (2001) 162501.
- [12] J. Jolie, P. Cejnar, R.F. Casten, S. Heinze, A. Linnemann, V. Werner, Phys. Rev. Lett. 89 (2002) 182502; P. Cejnar, *ibid.* 90 (2003) 112501.
- [13] P. Cejnar, S. Heinze, J. Jolie, Phys. Rev. C 68 (2003) 034326.
- [14] A. Volya, V. Zelevinsky, Phys. Lett. B 574 (2003) 27.
- [15] C. Emary, T. Brandes, Phys. Rev. Lett. 90 (2003) 044101; Phys. Rev. E 67 (2003) 066203; N. Lambert, C. Emary, T. Brandes, Phys. Rev. Lett. 92 (2004) 073602.
- [16] V. Zelevinsky, A. Volya, Phys. Rep. 391 (2004) 311.
- [17] C.N. Yang, T.D. Lee, Phys. Rev. 87 (1952) 404; 87 (1952) 410.
- [18] S. Grossmann, W. Rosenhauer, Z. Phys. 207 (1967) 138; 218 (1969) 437; S. Grossmann, V. Lehmann, Z. Phys. 218 (1969) 449.
- [19] P. Borrmann, O. Mülken, J. Harting, Phys. Rev. Lett. 84 (2000) 3511; O. Mülken, H. Stamerjohanns, P. Borrmann, Phys. Rev. E 64 (2001) 047105.
- [20] M.R. Zirnbauer, J.J.M. Verbaarschot, H.A. Weidenmüller, Nucl. Phys. A411 (1983) 161.
- [21] P.E. Shanley, Ann. Phys. 186 (1988) 292.
- [22] W.H. Steeb, W.D. Heiss, Phys. Lett. A 152 (1991) 339.
- [23] W.D. Heiss, W.-H. Steeb, J. Math. Phys. 32 (1991) 3003.

- [24] W.D. Heiss, M. Müller, I. Rotter, *Phys. Rev. E* 58 (1998) 2894.
- [25] W.D. Heiss, H.L. Harney, *Eur. Phys. J. D* 17 (2001) 149.
- [26] F. Iachello, A. Arima, *The Interacting Boson Model* (Cambridge University Press, Cambridge, UK, 1987).
- [27] A. Leviatan, A. Novoselsky, I. Talmi, *Phys. Lett. B* 172 (1986) 144.
- [28] F.J. Dyson, *J. Math. Phys.* 3 (1962) 140; B. Jancovici, *Phys. Rev. Lett.* 46 (1981) 386.
- [29] P. Pechukas, *Phys. Rev. Lett.* 51 (1983) 943; T. Yukawa, *ibid.* 54 (1985) 1883.